Available online at www.sciencerepository.org

Science Repository

Research Article

Histomorphometric and Radiographic Analysis of Biological Responses Following the Use of Pure Hydroxyapatite and Hydroxyapatite with Collagen

Fábio Aníbal Jara Goiris[1], Sandra Regina Masetto Antunes[1], Fábio André dos Santos[1], Eduardo Bauml Campagnoli[1], Juliana Larocca de Geus[2*], Edson Durval Menezes Alves[3], Érika de Lara[1], Matheus Tadao Wakasugui[1], Roberto Nakakogue[1] and Michel Fleith Otuki[4]

[1]*State University of Ponta Grossa, Ponta Grossa, Paraná, Brazil*

[2]*Department of Endodontics, Paulo Picanço School of Dentistry, Fortaleza, Ceará, Brazil*

[3]*Department of Implant Dentistry, São Leopoldo Mandic Post Graduate Center, Campinas, São Paulo, Brazil*

[4]*Department of Biochemistry, Federal University of Paraná, Curitiba, Paraná, Brazil*

ARTICLE INFO

Article history:

Received: 10 March, 2020

Accepted: 24 March, 2020

Published: 31 March, 2020

ABSTRACT

Background and Objectives: The objective of this study was to evaluate in vivo two new biomaterials for bone substitution aiming to determining their ability to enable bone neoformation in critical-size defects in rats' calvaria.

Methods: Synthetic hydroxyapatite were developed – Pure hydroxyapatite (HaP) and Hydroxyapatite with collagen (HCol). The third synthetic hydroxyapatite used as a comparing element was the commercial hydroxyapatite Alobone® (HaAl). Sixty Wistar rats divided randomly into four groups (Group 1, HaP; Group 2, HaCol; Group 3, HaAl and Group 4, Control). Critical size defects of 8mm were performed in the calvaria, and the three biomaterials were implanted. All groups also received a collagen membrane.

Results: On day 30, the inflammatory response on the defect was practically absent in all groups, mainly when compared to the period of 7 days. Some areas of bone neoformation were seen. There was predominance of osteoblasts, osteocytes, and macrophages in lower amounts. Regarding the radiographic aspect, after 30 days, a marked biodegradation of the hydroxyapatite and signs of bone neoformation were observed.

Conclusions: It was concluded that the results of our study in vivo can be used as a preliminary source of information about biocompatibility, biodegradability, and bone neoformation from the implant of new biomaterials in vivo.

Introduction

The application of substitutes in injuries or defects that compromise human bone tissue has been the subject of intense research, especially since the meeting organized in Geneva by the WHO in 2000: 'Decade of Bone and Articulation', where the effectiveness of multidisciplinary sought to overcome the limitations and complications resulting from bone substitutions and grafts [1]. Incorporating the designation of tissue engineering or, more specifically, Bone Tissue Engineering, research, especially in Periodontics and Implantology, has also been developing the use of cell therapy as an alternative for regenerative techniques [2-4]. The most common model used is to try to modulate the host's tissue response; or by the use of biomaterials, alone or through the in vivo implantation of cells cultured in vitro and transported in carrier materials, such as collagen and hydroxyapatite.

Considering its similarities in terms of chemical composition and properties compared to natural bone, hydroxyapatite (HA) has been widely used as a bone substitute, among other applications. Porous hydroxyapatite should fulfill the following requirements for the

[*]*Correspondence to: Juliana Larocca de Geus, Paulo Picanço School of Dentistry, Joaquim Sá, 900, Fortaleza, CE, Brazil, 60135 218; Tel: 558532723222; E-mail: juliana.degeus@facpp.edu.br*

http://dx.doi.org/10.31487/j.DOBCR.2020.01.09

formation of a suitable osteoconductive scaffold in bone regeneration: biocompatibility, osteoconductivity, interconnected porous structures, mechanical strength, and biodegradability. These factors provide an appropriate strategy for bone tissue engineering that is called "osteoconductive porous scaffold", which acts in combination with osteoinductive and osteogenic molecules or cells [5]. The compound of pure hydroxyapatite plus collagen (HaCol) would have the advantage that natural polymers such as gelatin, alginate, and chitosan can minimize both the toxicity of the biomaterial in its pure state and the chronic inflammation itself. In addition, collagen is a naturally occurring, highly biocompatible polymer, slightly irritating to the body and easily biodegradable [6].

In vivo experiments using laboratory animals predominate in the set of studies with biomaterials, generally identified as basic or preclinical experiments. These investigations are necessary not only for future applications in humans, but also because they provide decisive biological data, especially on new materials for dental specialties [7]. The aim of this study was to analyze the biological behavior of two forms of hydroxyapatite that were developed by the Chemistry Department of the State University of Ponta Grossa (UEPG), pure hydroxyapatite and hydroxyapatite with collagen and compared them to a form of hydroxyapatite that is already commercially available - Alobone®, by using a critical size defects model in the calvaria of rats with histomorphometric and radiographic analysis.

Materials and Method

I Obtaining and Characterizing the Biomaterial

The hydroxyapatite powder was obtained by the precipitation method, combining H_3PO_4 (Nuclear P.A. 85%) with Ca $(OH)_2$ (Vetec, P.A. 95%) at a molar Ca/P ratio of 1.67 in an aqueous medium. After the acid solution was added, the pH was adjusted to 10 with NH_4OH (Reatech, P.A. 28%) [8]. The precipitate was aged for 76 h, filtered under vacuum, and the resultant precipitate of each sample was dried in an oven at 100ºC for 24 hours. The hydroxyapatite obtained using this method had a nanocomposite structure (particles) and an average below 50 nm, whereas the particle agglomerates had an average that ranged from 6 to 9 micrometers. Other authors used mechanical methods to obtain a similar nanocrystalline hydroxyapatite with crystallite size in the range of 22 nm to 39 nm [9]. In our research, bovine collagen was added and solubilized in water by the ultrasound method for one hour and then lyophilized. The samples were characterized by X-ray diffraction (XRD) and scanning electron microscopy with field emission (EG-SEM).

II Analysis of Biocompatibility

This study used 60 rats, which were divided into four groups. The following three types of materials were placed in the calvaria of 45 of the rats: pure hydroxyapatite, hydroxyapatite with collagen, and commercial hydroxyapatite (Alobone®). A group of 15 rats was used as control, and the biomaterials were not used with these animals. The results indicated that the three biomaterials were biocompatible. New bone formation was also evident.

The rats were of the *rattus norvegicus albinus* species and the Wistar variety. The animals were aged around three months, and their body weight ranged from 250 to 300 grams. They were randomly distributed in different groups. The animals were sacrificed (each group, n = 15) at 7, 15, and 30 days to verify the biological behavior of the tissues and cells around the implanted biomaterial. The surgical procedures were performed at the Oral Pathology Laboratory of the Department of Dentistry at UEPG, and the biopsied specimens were processed and stained at the Medical Pathology Laboratory of the city of Ponta Grossa. The research project was approved by the Ethics Committee on Animal Use at the State University of Ponta Grossa (UEPG) in accordance with Process CEUA 22/2012, UEPG Protocol, 08258/2012. A pilot study was performed before the experiment to determine the ideal anesthetic for the animals, to practice the surgical procedures, and to determine the surgical protocol, including biopsies.

III Surgical Procedure and Post-Operative Care

The animals underwent general intraperitoneal anesthesia (IP) using 100 mg/ml ketamine, (injectable general anesthetic based on 1.16 g hydrochloride ketamine, 10 ml, Ceva Brasil®) by dilution of 3.75 ml of this ketamine solution together with the muscle relaxant xylazine, 100 mg/ml (xylazine, 200 mg; 10 ml bottle, veterinary use, imported, Hertape Calier®), at a ratio of 0.5 ml of xylazine diluted in 5.75 ml of distilled water. Each animal was administered with 0.2 ml per 100 g weight. The use of ketamine, together with xylazine produced anesthesia and sedation in the animals within 30-40 minutes [10].

This study used 60 female rats (n=60), in which the following three different biomaterials were implanted: pure hydroxyapatite (UEPG); hydroxyapatite-collagen (UEPG); and commercial hydroxyapatite (Alobone®). The animals were randomly divided into the following four groups for treatment, based on calvarial defect filling material: 1) Ha-Alobone® group (n = 15); 2) Pure Ha group (n = 15); 3) Ha-collagen group (n = 15); and 4) Control group (n = 15), which used no type of filling material. After anesthesia, the trichotomy of the frontoparietal region of the animal's head was performed using an electric shaving appliance and local asepsis using 10% povidone-iodine. A triangular format was used to perform a mucoperiosteal incision with a No. 15 razor scalpel in the calvaria of the rats. A Molt peristome and a nº 1 Ochsenbein (SS WHITE) chisel were used to ensure that the full thickness of the flaps was obtained and that the cortical bone of the region was completely exposed.

Bicortical, full-thickness, critical defects were created in the frontoparietal region of each animal using an 8.0mm outer diameter trephine. The critical size defect with trephine was performed with sufficient irrigation using saline. The physical barrier placed over the critical defect consisted of a *Heli Tape* (Integra Life Sciences Corporat®, USA) absorbable collagen wound dressing. The dura under the critical defect was obligatorily kept intact (Figure 1A). After removal of the outer and inner cortical strips, the critical defects (8.0 mm diameter) were only filled with blood clot and only with collagen membrane (for the control group). In the experimental groups, the defects were filled with biomaterials, and then collagen membranes were put in place (Figures 1B & 1C).

Then the flaps were repositioned using No. 3 black silk thread (Ethicon, Johnson & Johnson, São Paulo, SP, Brazil) sutures. The animals showed

no bleeding or any other systemic condition that could exclude them from the study.

After the surgical procedures, the animals received analgesic, and anti-inflammatory ketoprofen (IP) that was injected in a single dose at a ratio of 2 mg/kg, and they were placed in special cages (exposed to low light) to recover from the anesthesia. The temperature in the immediate post-operative environment ranged from 27 to 30°C to avoid hypothermia. The immediate consumption of water was monitored to prevent dehydration. In the following days, the food was regular, and the administration of water was ad libitum. There was no postoperative death of the animals.

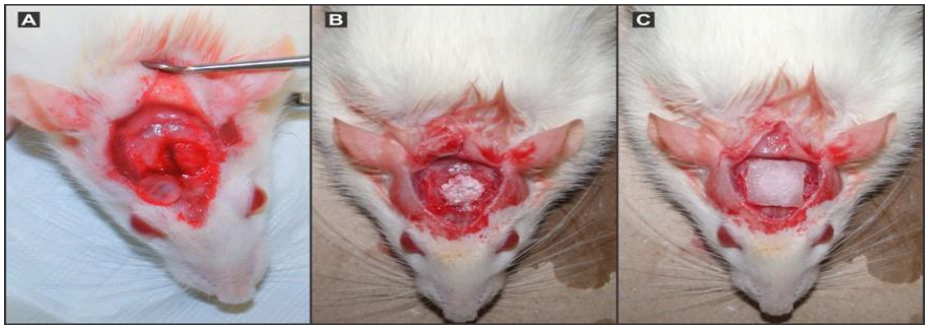

Figure 1: In **(A)** after careful removal (to prevent damage to the dura) of the outer and inner cortical strips, the critical defects (8.0 mm diameter- see the cortical cover pointed to by an arrow). In **(B)**, the defects were filled with biomaterials; in **(C)** collagen membranes were put in place, and then flaps were carefully sutured.

IV Obtaining Biopsies and Histotechnical Preparation

The animals (n = 15 for each period) were sacrificed at 7, 15, and 30 days after surgery by an overdose of isoflurane - 240 ml bottle - (inhalation solution indicated in humans for the induction and maintenance of general anesthesia). Under the effect of isoflurane, each animal underwent cervical dislocation with a metal bar in order to confirm euthanasia. The biopsies of the frontoparietal region of the animals were performed in line with the following routine: trichotomy and using a disc-shaped rotary tool under low speed to remove the frontoparietal bone of the animals. The biopsies were fixed in 4% formalin that was buffered for 48 hours. The biopsies were decalcified with EDTA to 7% for 21 days.

V Histotechnical Procedure and Histomorphometric Analysis

The decalcified tissue was submitted to the standard procedure for histotechnical staining - hematoxylin and eosin. The pieces were placed in a paraffin block for the cutting by microtome (approximately 5-7 mm thickness). The slides were analysed (by a single professional), and a descriptive and semi-quantitative analysis was performed. The numerical correlation references adopted for the presence or absence of those parameters were as follows: osseous repair, connective tissue repair (presence of collagen fibres) and inflammatory infiltrate (predominance of a particular type of inflammatory cell): 0 = absent; 1 = mild; 2 = moderate; 3 = severe [11].

VI Radiographic Processing and Analysis

Radiographic processing and analysis of standardized radiographic images of the rat calvaria gross specimens were obtained using a dental radiographic unit (70 kVp, 7mA for 1s; Gendex 770, Gendex Corporation, Des Plaines, IL, USA) and No. 2 Kodak Ultra-speed X-ray film (Eastman Kodak Company, Rochester, NY, USA). The calvaria gross specimens, recorded individually, were placed on the radiographic film, the defect area placed flat on the film, and the X-ray source directed perpendicular to the film/gross specimen. The X-ray source-film distance was 12 in. Radiographs were processed in an automatic dental film processor (A/T 2000, Air Techniques, Hicksville, NY, USA).

The radiographs (analog films) were transformed into digitized images using a film scanner (620ST AcerScan, San Jose, CA, USA) at 1200 dpi, which was connected to a standard PC. The defects were classified and scored according to the following criteria related to the defect margins: 0=No/limited bone fill; 1=Partial bone fill, and 2=Complete bone fill [12]. In our research we performed the design of the critical bone defect ('critical size defects') with a circle, as carried out on digital radiographs of rats' calvaria. The same and only observer analyzed the images, which had been used in the Kappa system of the histological analysis to distinguish the different radiographic scores – 0, 1, and 2 [13].

VII Statistical Analysis

Data were statistically analyzed using the Non-Parametric Kruskal–Wallis test with Dunn's test (for multiple comparisons) to study the subcutaneous tissue response to different biomaterials. Statistical analysis was performed with IBM® SPSS® (SPSS Inc., IBM Corporation, NY, USA) Statistics Version 21 for Windows. The significance levels observed, as indicated by an asterisk in the figures, were considered statistically significant at $p < 0.05$.

Results

Figure 2 shows the inflammatory response at 7, 15, and 30 days for all the groups. Figure 3 illustrate the histopathology of the experimental groups, and the (Figure 4) show radiographic findings. The results showed no significant differences between the groups when they were compared at each of the evaluated time periods. In terms of the same group at different time periods, the inflammation at seven days was highest, reducing by day 15 (with no significant difference); there was also no significant difference between 15 and 30 days. However, the differences were significant for the values between seven and 30 days. This behaviour was observed in all the groups.

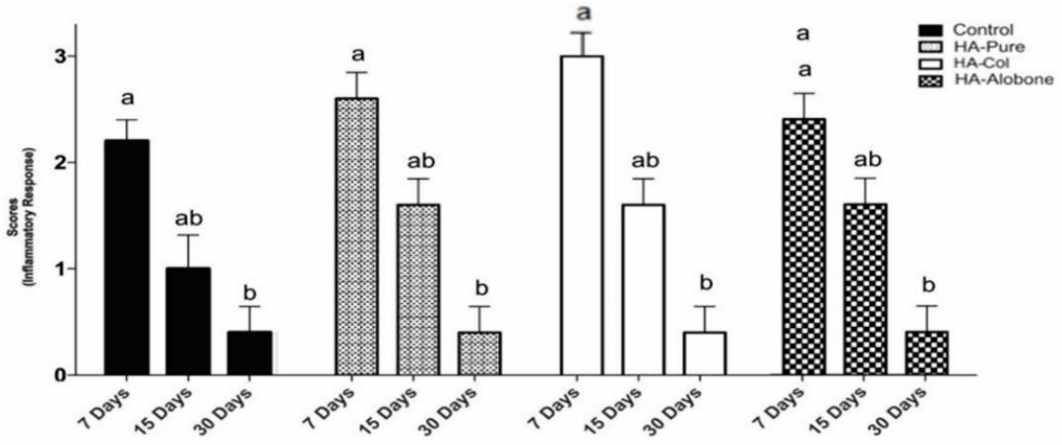

Figure 2: Comparison between different groups at each time point (Kruskal-Wallis test); p> 0.05, no significant difference. Comparison between different times in the same group (Kruskal-Wallis test with Dunn's post test) Different letters (p <0.01, significant) for biomaterials.

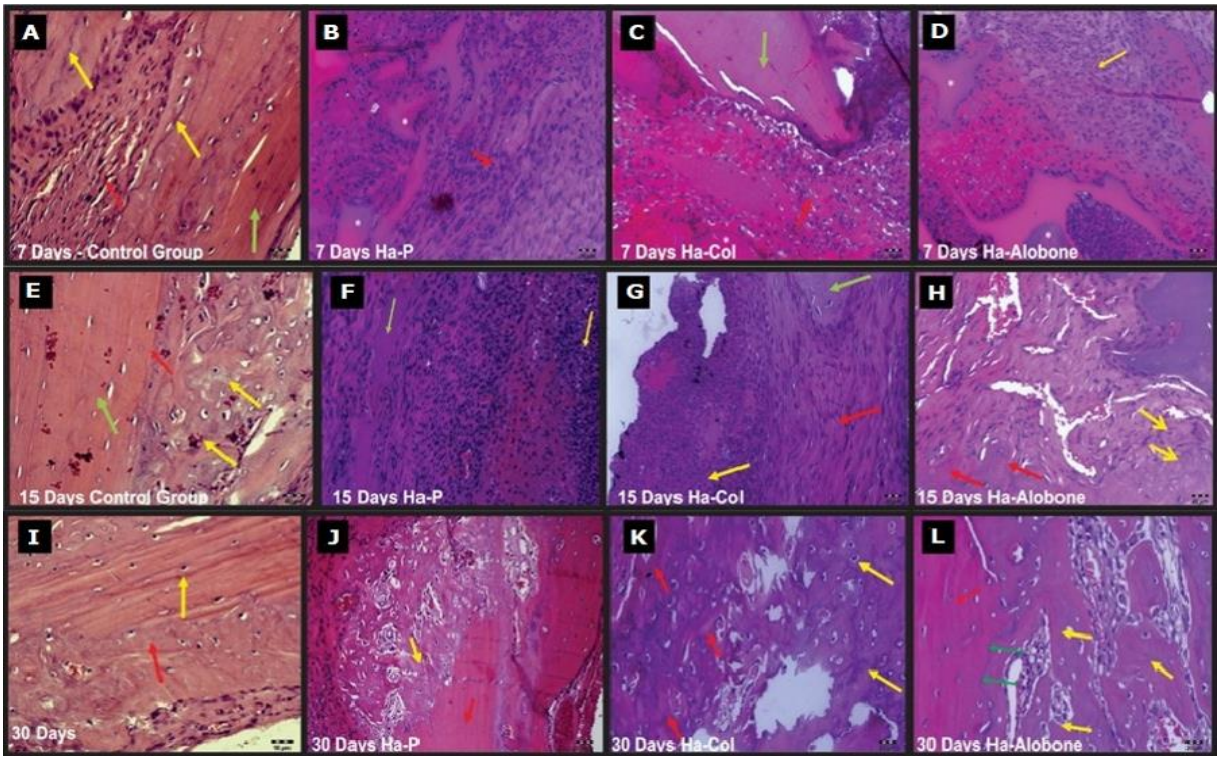

Figure 3: Control Group, 7 days: In **(A)** early bone formation (yellow arrows) and organized collagen tissue (red arrow). The pre-existing mature bone had lamellae characteristics (green arrow). (Images HE 400X). **HaP, 7 days**: In **(B)** dense inflammatory infiltrate with neutrophils and macrophages. The biomaterial was dispersed in the connective tissue (asterisks). Granulation tissue was present (red arrow). **HaCol, 7 days**: In **(C)** dense inflammatory infiltrate with neutrophils and macrophages. The biomaterial appeared in the conjunctive tissue (asterisk). The presence of granulation tissue (red arrow) was observed. Note the pre-existing mature bone tissue (green arrow). **HaAlobone, 7 days**: In **(D)** dense inflammatory infiltrate with neutrophils and macrophages. The biomaterial (*) was dispersed in the connective tissue. Granulation tissue (yellow arrow) was observed. **Control Group, 15 days**: In **(E)**, extensive bone formation (yellow arrows). The pre-existing mature bone had characteristics of lamellae (green arrow) and cement lines (red arrow). There were no signs of inflammation. (Images HE 400X). **HaP, 15 days**: In **(F)**inflammatory infiltrate and granulation tissue (yellow arrow). There was osteoid formation (green arrow). **HaCol, 15 days**: In **(G)** granulation tissue (yellow arrow). Organized collagenous tissue was present (red arrow). New bone formation appeared amid the organized collagen (green arrow). **HaAlobone, 15 days**: In **(H)** a clear decrease in the inflammatory infiltrate and increased deposition of collagen fibers in the granulation tissue. Signs of new bone formation (red arrows) and the formation of osteoid (yellow arrows). **Control Group, 30 days**: In **(I)** perfect inter-relationship between mature bone or pre-existing bone (yellow arrow) and the newly formed bone (red arrow). No sign of inflammation was observed. (Images HE 400X). **HaP, 30 days**: In **(J)** clear new bone formation with a predominance of osteoblasts (yellow arrow). The pre-existing old bone showed typical lamellae (red arrow). There were no signs of inflammation.**HaCol, 30 days**: In **(K)** large area of new bone formation. The presence of larger areas of calcification (red arrows) and areas of less calcification (yellow arrows). No further inflammatory process was observed. **HaAlobone 30 days**: In **(L)** the absence of inflammatory infiltrate. Newly formed bone (yellow arrows) predominated. The pre-existing old bone (red arrow) showed cement lines (green arrows) in contact with the new bone. Osteoblasts and osteocytes were the predominant cells.

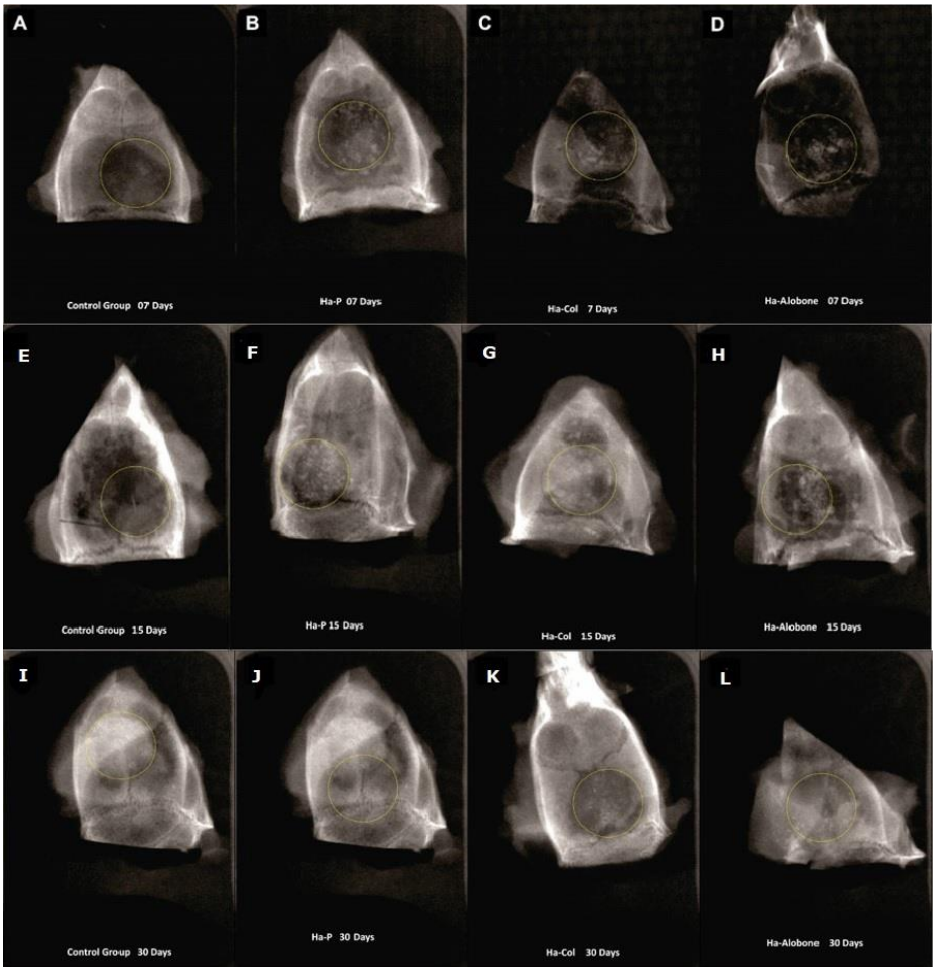

Figure 4: Control Group, 7 days: In **(A)**, a radiolucent area is observed (in the center of the circle) and the biomaterial is dispersed, but there was early new bone formation on the margins of the critical defect. No biomaterial was used in this group, only collagen membrane. **HaP, 7 days**: In **(B)**, the material was dispersed in the area of the critical defect, and there were radiolucent areas, which were typical of inflammation. **HaCol, 7 days**: In **(C)**, radiolucent image in the area of the critical defect. The biomaterial was dispersed. **HaAlobone, 7 days**: In **(D)**, dispersed material in the critical defect, and even in adjacent areas. Extensive radiolucent areas were present, which corresponded to the granulation tissue. **Control Group, 15 days**: In **(E)**, there was extensive new bone formation from the margins of the critical defect. However, there were still areas with radiolucent images. **HaP, 15 days**: In **(F)** new bone formation within the critical defect, but with radiolucent areas and dispersed material. **HaCol, 15 days**: In **(G)**radiolucent areas, but new bone formation was present. The material remained dispersed inside and outside the critical defect. **HaAlobone, 15 days**: In **(H)** a decrease in the radiolucent area compared to what was observed at seven days. New bone formation was present on the margins of the critical defect. Material was dispersed in the critical defect. **Control Group, 30 days**: In **(I)**, there was extensive new bone formation from the margins of the defect. No radiolucent areas were observed. **HaP, 30 days**: In **(J)** new bone formation within the critical defect, but with radiolucent areas. Little dispersed material. **HaCol, 30 days**: In **(K)** radiolucent areas, but there was evident new bone formation. A small portion of the material remained dispersed within the critical defect. **HaAlobone 30 days**: In **(L)**, there was a decrease in the radiolucent area. New bone formation was present on the margins of the critical defect, but there was still dispersed material in the defect

I Seven Days

In the first week after surgery, an increase was observed in the values for inflammation in all the groups. Neutrophils and macrophages were present in all the groups, and the biomaterial was dispersed in the area of the critical defect. Granulation tissue was present in all the groups (Figure 3).

II Fifteen Days

At this time, there was a decrease in the inflammatory response in all the groups. The control group, which only contained collagen membrane, showed the highest reduction in inflammation. The increased formation of collagen tissue was observed within the granulation tissue. The development of new blood vessels in the developing granulation tissue was observed. Osteoblasts and macrophages were the predominant cells (Figure 3).

III Thirty Days

There was a significant decrease in the inflammatory response in all the groups, especially when compared to the seven-day period. There were extensive areas of new bone formation. There was a predominance of osteoblasts, osteocytes, and macrophages but in lower quantities. The

mature bone tissue showed cement lines in contact with the new bone (Figure 3).

IV Radiographic Results

Regarding radiographic results, the correlation between histological scores considering collagen fibers, inflammatory infiltrate (0 = absent; 1 = discrete; 2= moderate; 3 = intense), according to Mendonça *et al.* (2007); and the x-ray analysis scores – 0, 1 and 2, according to Pryor *et al.* (2006), can be seen in (Table 1) [11, 12]. The results of the correlation between histological and x-ray scores show that there was a negative correlation. This means that when one of the variables increases, the other decreases. In such a case, we understand that from the moment the inflammatory response scores decrease, the tissue recovery with radiographic bone neoformation increases. Therefore, with the inflammation reduction, the increase in bone formation in the region of the bone defect starts to occur (Figure 4).

Discussion

Hydroxyapatite is the main inorganic calcium phosphate mineral component in bones and teeth. This research used a porous hydroxyapatite (Pha), which is a material with faster resorption and is more osteoconductive than dense Ha (Dha). It has been used in many experimental and clinical trials as material for artificial bone grafts. In the case of Pha, extracellular fluid induces disintegration of the ceramic granules, allowing the gradual growth of bone tissue into the spaces among them without the interposition of fibrous tissue [14, 15]. The synthetic biomaterial used in our research was also a nanocrystalline hydroxyapatite (nHAp) with a particle size smaller than 50 nm. According to Sun, Zhou, and Lee, nHAp can be combined with various types of bioactive polymers to generate highly porous biocomposite materials that are used for osteoconduction [16]. The benefits of synthetic grafts include their availability, sterility and reduced morbidity.

The aim of this study was to evaluate the reaction of tissues to two types of synthetic hydroxyapatites (HaP and HaCol), which were produced by UEPG, and to compare them to a third type, which was the standard (HaAlobone®). In our study, there was no significant difference between pure hydroxyapatite (HaP) and hydroxyapatite with collagen (HaCol) in relation to inflammatory response, biocompatibility, new bone formation, and the biodegradability of the material deployed in a critical defect in the calvaria of rats. In conjunction with previous reports about in vivo bone regeneration] the results of the present study have shown that the histological response could be used as a preliminary source of information regarding the biocompatibility and biodegradability of material implanted in the calvaria of rats [7-22].

The implantation of biomaterials in the critical calvarial defect of rats has been widely accepted as an important test to assess biocompatibility, biodegradability, and osseous healing. An 8mm diameter calvaria osteotomy defect has been suggested as being suitable to assess specific biomaterial for bone regeneration, and it constitutes a critical-size defect in the rat [23]. Defects of a size that will not heal during the lifetime of the animal are termed critical size defects (CSDs). In fact, animal models, and more specifically rodent models, have been extensively used and have contributed greatly to the development and establishment of a wide range of translational approaches designed to regenerate bone tissue [24, 25].

Regarding inflammatory response and bone formation, our research results showed no significant differences between the groups when they were compared in each of the periods that were assessed. The differences were significant for values between seven and 30 days. This behaviour was observed in all the groups. At seven days, there was an increase in the values for inflammation in all groups. Neutrophils and macrophages were present in all the groups, and biomaterial was dispersed in the area of the critical defect. Granulation tissue was present in all the groups. At 15 days, this granulation tissue allowed the formation of collagen fibers inside the tissue, which started the osteoid formation process. New blood vessels also appeared. Macrophages, multinucleated giant cells and osteoblasts predominated in this period.

At thirty days, there was a significant decrease in the inflammatory response in all the groups compared to the situation at seven days. New bone formation was evident and extensive. Bone regeneration mainly depends on the activity of pre-osteoblastic cells and various mechanisms that regulate their proliferation and differentiation. The establishment of a blood vessel network by vasculogenesis and angiogenesis is essential for cellular gaseous exchange, nutrient supply and waste product removal during new tissue formation [26].

Wang, Gerstenfeld, and Glimcher and Alexander noted that in the calvaria of mice there was little evidence that ossification occurred through the classical sequence of endochondral mineralization, which is perceived as an intra-membranous type of calcification where, in the presence of granulation tissue, stem cells begin a process of regeneration to differentiate into osteogenic cells [27, 28]. In our study, at seven days all the groups presented granulation tissue. This tissue dwindled and finally disappeared as the presence of collagen fibers and osteoid tissue intensified. Al-Hezaimi *et al.* evaluated the potential of bone marrow-derived mesenchymal stem cells (BMSCs) to regenerate bone in an established rat calvarium model in real-time [21].

The evidence of new bone formation (NBF) treated with BMSCs appeared as early as two weeks. Similarly, in our study, the new formation of bone tissue in the critical defect of calvaria in rats also began around 15 postoperative days. Calcification increased with time, and at 30 days, there was extensive formation of bone within the defect. The results of an experimental study also found that by the 14th day of cellular differentiation, calcium and phosphate deposition had started, thereby forming new mineralized tissues. At the same time, the authors observed that there was a synergistic relationship between osteocytes and osteoblasts in producing biochemical signals to stimulate the osteogenic differentiation of mesenchymal stem cells (MSCs) [29]. In fact, osteoblasts, differentiated from MSCs, secrete the organic bone matrix and induce mineralization.

In critical defects produced in rat calvaria, one of the original sources of MSCs is the periosteum that remains around the defect [30]. Dimitriou, Tsiridis, and, Giannoudis indicated that during fracture healing, potential sources of stem cells include bone marrow, granulation tissue, the deep layer of the periosteum, the endosteum, and the surrounding soft tissues [31]. Furthermore, perivascular mesenchymal stem cells that exist in blood vessel walls contribute to fracture or can the healing of osseous

damage. During this form of osseous repair, initially, the hematoma is formed, and then inflammation occurs. The major factors at this initial inflammatory phase include cytokines, platelets, bone morphogenetic proteins (BMPs), and mesenchymal stem cells (MSCs).

This form of bone tissue healing has been associated with the presence of macrophages, which, together with fibroblast cells, are typical components of granulation tissue [11]. Inflammatory monocytes and tissue-resident macrophages are key regulators of tissue repair, regeneration, and fibrosis [32]. In our study, the biodegradability of the material was evident (verified through histopathological data and radiographic images), and it was attributed in part to macrophage activities, which fused to form multinucleated giant cells. At 30 days very little material was still present inside the critical bone defect. In relation to macrophages, Loi *et al.* [33] found that there was a population of bone-specific resident macrophages named osteomacs residing in the periosteum and endosteum, which participated in the regulation of fracture healing. Osteomacs were specifically associated with sites of intramembranous bone deposition.

With regard to the radiographic findings of this study, Pryor *et al.* found that radiographic evaluations of the healing process of critical-size calvaria osteotomy defects had the potential advantage of being less costly and time-consuming than the "gold standard" protocol of histologic analysis; however, their validity has not been fully explored [34]. When no/limited and partial bone fill occurred, the radiographic analysis tended to overestimate bone fill, and underestimate bone fill when complete closure of the defect sites was observed in the histological analysis. The authors concluded that radiographic evaluations of bone fill in rat calvaria osteotomy defects yielded a low level of accuracy [34]. The evaluation of bone formation in animal models aimed at treatment recommendations for clinical application should not be solely based on radiographic analysis but should be confirmed using histologic observations.

In our study, the radiographic images of critical-size calvaria osteotomy defects showed proper agreement between the histologic and radiographic visual analysis (by using scores of 0, 1 and 2), especially in the first post-operative week, when there were extensive radiolucent images in the bone defect area and great bone formation (radiopaque images) at 30 days [12]. The use of radiographs in our study was also useful to detect the presence and distribution of biomaterials inside the critical defect at the studied times. The implanted biomaterial did not wholly disappear at 30 postoperative days. During this period, there was plenty of new bone formation, but some of the material remained inside the critical defect.

This occurred in all the experimental groups. On the other hand, multiple methodologies, including histological analysis, electron microscopy, and radiological techniques, have reported relevant and complementary data, with proven adequacy, in the assessment of bone repair/regeneration process [35]. Finally, this study presents some limitations. The concept that animal research, particularly that relating to pharmaceuticals and environmental agents, maybe a poor predictor of human experience is not new [36]. Due to this limitation, further studies must be carried out in humans.

Conclusion

Based on the results of this study, it can be concluded that the pure hydroxyapatite and hydroxyapatite with collagen that were produced at the State University of Ponta Grossa (UEPG) and were tested in Critical-Sized Rat Calvarial Defects showed biodegradability, biocompatibility and promoted new bone formation. There were no significant differences between the biomaterials that were tested regarding biocompatibility and biodegradability. Compared with the standard hydroxyapatite (HaAlobone®), the two types of hydroxyapatite produced by UEPG did not show significant differences in terms of in vivo biological behavior.

Acknowledgements

The authors acknowledge the Fundação Araucária for the financial support.

References

1. Kawashi EY, Reis RR, Alves OL (2000) Biocerâmicas: tendências e perspectivas de uma área interdisciplinar. *Quim Nova* 23: 518-522.
2. Amini AR, Laurencin CT, Nukavarapu SP (2012) Bone tissue engineering: recent advances and challenges. *Crit Rev Biomed Eng* 40: 363-408. [Crossref]
3. Chen FM (2017) [Periodontal tissue engineering and regeneration]. *Zhonghua Kou Qiang Yi Xue Za Zhi* 52: 610-614. [Crossref]
4. Shanbhag S, Pandis N, Mustafa K, Nyengaard JR, Stavropoulos A (2018) Bone tissue engineering in oral peri-implant defects in preclinical in vivo research: A systematic review and meta-analysis. *J Tissue Eng Regen Med* 12: e336-e349. [Crossref]
5. Yoshikawa H, Myoui A (2005) Bone tissue engineering with porous hydroxyapatite ceramics. *J Artif Organs* 8: 131-136. [Crossref]
6. Zhao HY, Wu J, Zhu JJ, Xiao ZC, He CC et al. (2015) Research Advances in Tissue Engineering Materials for Sustained Release of Growth Factors. *Biomed Res Int* 2015: 808202. [Crossref]
7. da Silva Morais A, Oliveira JM, Reis RL (2018) Small Animal Models. *Adv Exp Med Biol* 1059: 423-439. [Crossref]
8. Kosachan N, Jaroenworaluck A, Jiemsirilers S, Jinawath S, Stevens R (2017) Hydroxyapatite nanoparticles formed under a wet mechanochemical method. *J Biomed Mater Res B Appl Biomater* 105: 679-688. [Crossref]
9. Silva CC, Pinheiro AG, Miranda MAR, Góes JC, Sombra ASB (2003) Structural properties of hydroxyapatite obtained by mechanosynthesis. *Solid State Sciences* 5: 553-558.
10. Mezadri TJ, Amaral VLL (2004) Anestesia e analgesia em animais de laboratório. In: Animais de laboratório: cuidados na iniciação experimental, Editora da UFSC. *Florianopólis* 101-130.
11. Mendonça R, Freitas AC, Ramalho LP, Farias JG, Ribeiro MM (2007) Avaliação Histológica do Processo de Reparo Ósseo Após Implantação de BMPs. *Pesq Bras Odontoped Clin Integr* 7: 291-296.
12. Pryor ME, Susin C, Wikesjo UM (2006) Validity of radiographic evaluations of bone formation in a rat calvaria osteotomy defect model. *J Clin Periodontol* 33: 455-460. [Crossref]
13. Roh J, Kim JY, Choi YM, Ha SM, Kim KN et al. (2016) Bone Regeneration Using a Mixture of Silicon-Substituted Coral HA and β-TCP in a Rat Calvarial Bone Defect Model. *Materials (Basel)* 9: E97. [Crossref]

14. Kwon BJ, Kim J, Kim YH, Lee MH, Baek HS et al. (2013) Biological advantages of porous hydroxyapatite scaffold made by solid freeform fabrication for bone tissue regeneration. *Artif Organs* 37: 663-670. [Crossref]
15. Andrade JC, Camilli JA, Kawachi EY, Bertran CA (2002) Behavior of dense and porous hydroxyapatite implants and tissue response in rat femoral defects. *J Biomed Mater Res* 62: 30-36. [Crossref]
16. Sun F, Zhou H, Lee J (2011) Various preparation methods of highly porous hydroxyapatite/polymer nanoscale biocomposites for bone regeneration. *Acta Biomater* 7: 3813-3828. [Crossref]
17. Marden LJ, Hollinger JO, Chaudhari A, Turek T, Schaub RG et al. (1994) Recombinant human bone morphogenetic protein-2 is superior to demineralized bone matrix in repairing craniotomy defects in rats. *J Biomed Mater Res* 28: 1127-1138. [Crossref]
18. Winn SR, Schmitt JM, Buck D, Hu Y, Grainger D et al. (1999) Tissue-engineered bone biomimetic to regenerate calvarial critical-sized defects in athymic rats. *J Biomed Mater Res* 45: 414-421. [Crossref]
19. Dupoirieux L, Pourquier D, Picot MC, Neves M (2001) Comparative study of three different membranes for guided bone regeneration of rat cranial defects. *Int J Oral Maxillofac Surg* 30: 58-62. [Crossref]
20. Verna C, Dalstra M, Wikesjo UM, Trombelli L, Carles Bosch (2002) Healing patterns in calvarial bone defects following guided bone regeneration in rats. A micro-CT scan analysis. *J Clin Periodontol* 29: 865-870. [Crossref]
21. Al Hezaimi K, Ramalingam S, Al Askar M, ArRejaie AS, Nooh N et al. (2016) Real-time-guided bone regeneration around standardized critical size calvarial defects using bone marrow-derived mesenchymal stem cells and collagen membrane with and without using tricalcium phosphate: an in vivo micro-computed tomographic and histologic experiment in rats. *Int J Oral Sci* 8: 7-15. [Crossref]
22. Fang CH, Lin YW, Lin FH, Sun JS, Chao YH et al. (2019) Biomimetic Synthesis of Nanocrystalline Hydroxyapatite Composites: Therapeutic Potential and Effects on Bone Regeneration. *Int J Mol Sci* 20: E6002. [Crossref]
23. Spicer PP, Kretlow JD, Young S, Jansen JA, Kasper FK et al. (2012) Evaluation of bone regeneration using the rat critical size calvarial defect. *Nat Protoc* 7: 1918-1929. [Crossref]
24. Schmitz JP, Hollinger JO (1986) The critical size defect as an experimental model for craniomandibulofacial nonunions. *Clin Orthop Relat Res* 299-308. [Crossref]
25. Gomes PS, Fernandes MH (2011) Rodent models in bone-related research: the relevance of calvarial defects in the assessment of bone regeneration strategies. *Lab Anim* 45: 14-24. [Crossref]
26. Black CR, Goriainov V, Gibbs D, Kanczler J, Tare RS et al. (2015) Bone Tissue Engineering. *Curr Mol Biol Rep* 1: 132-140. [Crossref]
27. Wang J, Yang R, Gerstenfeld LC, Glimcher MJ (2000) Characterization of demineralized bone matrix-induced osteogenesis in rat calvarial bone defects: III. Gene and protein expression. *Calcif Tissue Int* 67: 314-320. [Crossref]
28. Alexander KA, Chang MK, Maylin ER, Kohler T, Muller R et al. (2011) Osteal macrophages promote in vivo intramembranous bone healing in a mouse tibial injury model. *J Bone Miner Res* 26: 1517-1532. [Crossref]
29. Birmingham E, Niebur GL, McHugh PE, Shaw G, Barry FP et al. (2012) Osteogenic differentiation of mesenchymal stem cells is regulated by osteocyte and osteoblast cells in a simplified bone niche. *Eur Cell Mater* 23: 13-27. [Crossref]
30. Einhorn TA (1998) The cell and molecular biology of fracture healing. *Clin Orthop Relat Res* 355: S7-S21. [Crossref]
31. Dimitriou R, Tsiridis E, Giannoudis PV (2005) Current concepts of molecular aspects of bone healing. *Injury* 36: 1392-1404. [Crossref]
32. Wynn TA, Vannella KM (2016) Macrophages in Tissue Repair, Regeneration, and Fibrosis. *Immunity* 44: 450-462. [Crossref]
33. Loi F, Cordova LA, Pajarinen J, Lin TH, Yao Z et al. (2016) Inflammation, fracture and bone repair. *Bone* 86: 119-130. [Crossref]
34. Pryor ME, Yang J, Polimeni G, Koo KT, Hartman MJ et al. (2005) Analysis of rat calvaria defects implanted with a platelet-rich plasma preparation: radiographic observations. *J Periodontol* 76: 1287-1292. [Crossref]
35. Notodihardjo FZ, Kakudo N, Kushida S, Suzuki K, Kusumoto K (2012) Bone regeneration with BMP-2 and hydroxyapatite in critical-size calvarial defects in rats. *J Craniomaxillofac Surg* 40: 287-291. [Crossref]
36. Bracken MB (2009) Why animal studies are often poor predictors of human reactions to exposure. *J R Soc Med* 102: 120-122. [Crossref]